

## Supporting Information

### Phosphorylation of Covalent Organic Frameworks Nanospheres for Inhibition of Amyloid- $\beta$ Peptide Fibrillation

Linli Yao,<sup>a</sup> Zhe Zhou,<sup>b</sup> Suxiao Wang,<sup>a</sup> Qichao Zou,<sup>a</sup> Hang-Xing Wang,<sup>\*a</sup> Li-Xin  
Ma,<sup>c</sup> and Shengfu Wang,<sup>a</sup> and Xiuhua Zhang<sup>\*a</sup>

[a] Collaborative Innovation Center for Advanced Organic Chemical Materials  
Co-constructed by the Province and Ministry, College of Chemistry and Chemical  
Engineering, Hubei University, Wuhan, 430062, China.

[b] Department of Neurology, The First Hospital of Lanzhou University, Lanzhou,  
730000, China

[c] State Key Laboratory of Biocatalysis and Enzyme Engineering, School of Life  
Science, Hubei University, Wuhan, 430062, China

Corresponding Authors:

Prof. Hang-Xing Wang (E-mail: [wanghx0917@163.com](mailto:wanghx0917@163.com)) and Xiuhua Zhang (E-mail:  
[zhangxh@hubu.edu.cn](mailto:zhangxh@hubu.edu.cn))

Table of Contents		Page
Experimental Procedures		1-5
Figures and Tables		6-28
Figure S1	TEM image and particle size distribution of TD-COFs	6
Figure S2	Energy-dispersive X-ray spectroscopy of SP-COFs	7
Figure S3	Illustration of the amino acids sequence of A $\beta$ <sub>42</sub> peptide	8
Figure S4	Time nodes-structure phase of A $\beta$ <sub>42</sub> peptide across the channel of SP-COFs in molecular dynamics process	10
Tables S1	Binding free energy of SP-COFs and A $\beta$ <sub>42</sub> complex	12
Figure S5	Steered molecular dynamics of the most stable phase of A $\beta$ <sub>42</sub> and single pore of SP-COFs when co-incubated	13
Figure S6	TEM images and DLS measurement of A $\beta$ <sub>42</sub> &SP-COFs mixtures	14
Figure S7	Zeta potential of A $\beta$ <sub>42</sub> and A $\beta$ <sub>42</sub> &SP-COFs	15
Figure S8	Fluorescence intensity change of ThT affected by SP-COFs co-incubation	16
Figure S9	The concentration changes of A $\beta$ <sub>42</sub> before and after mixing with SP-COFs	17
Figure S10	Fluorescence spectra of amino acids with ThT in PBS buffer solution	18
Table S2	Secondary structure analysis of A $\beta$ <sub>42</sub> content according to CD spectra	19
Figure S11	TEM images of SP-COFs after co-incubated with A $\beta$ <sub>42</sub> monomers in PBS buffer solution at 37 °C at different intervals (0 h, 24 h, 72 h, 96 h)	20
Figure S12	PXRD of SP-COFs after co-incubated with A $\beta$ <sub>42</sub> monomers in PBS buffer solution at 37 °C at different intervals (0 h, 24 h, 72 h, 96 h)	21
Figure S13	TEM images of SP-COFs in cell sap (0 h and 96 h)	22
Figure S14	Molecular structure, spectra of UV-Vis and PL, MS, and <sup>1</sup> H NMR of	23

	DMBPD	
Figure S15	The CLSM images of DMBPD&SP-COFs	24
Figure S16	The CLSM images of DMBPD&SP-COFs and A $\beta$ <sub>42</sub> (without labeling)	25
Figure S17	The CLSM images of FITC-A $\beta$ <sub>42</sub>	26
Figure S18	The CLSM images of DMBPD&SP-COFs and FITC-A $\beta$ <sub>42</sub>	27
Figure S19	The cytotoxicity experiments of other three kinds of cells including Hela, HUVECs, and A549 cells	28
References		29

# 1. Experimental Procedures

## 1.1 Chemicals and Apparatus.

All reagents and solvents were purchased from commercial sources and used without further purification. 1,3,5-Tris(4-aminophenyl) benzene (TPB) was obtained from Energy Chemical Ailan (Shanghai) Chemical Industry Technology Co., Ltd., and 2,5-dihydroxyterephthaldehyde (DHTP) was obtained from Energy Chemical. Thioflavin T (ThT) was purchased from Sigma. Acetic acid (HAc), tetrahydrofuran (THF), Sodium hydroxide (NaOH), Anhydrous acetonitrile (ACN), methyl alcohol (MeOH) phosphorus oxychloride ( $\text{POCl}_3$ ), 1,1,1,3,3,3-hexafluoro-2-propanol (HFIP) and 3-(4,5-dimethyl-2-thiazolyl)-2,5-diphenyl-2H-tetrazolium bromide (MTT) were obtained from Aladdin Industrial Corporation (Shanghai, China). Beta-Amyloid (1-42) ( $\text{A}\beta_{42}$ ), N to C : DAEFRHDSGYEVHHQKLVFFAEDVGSNKGAIIGLMVGGVVIA, and FITC- $\text{A}\beta_{42}$  (5-FITC-(Acp)-DAEFRHDSGYEVHHQKLVFFAEDVGSNKGAIIGLMVGGVVIA) were purchased from Suzhou Qiangyao Biotechnology Co., Ltd. (ChinaPeptides Co., Ltd.). All other chemical reagents were of analytical grade, and millipore ultrapure water with a certain resistivity  $>18.25 \text{ M}\Omega\text{-cm}$  was used throughout the experiment. The working solution was using a  $50 \mu\text{M}$  phosphate buffer solution (PBS,  $\text{pH}=7.40$ ).

Scanning electron micrographs (SEM) were measured on a LEO1530VP (Zeiss, Germany). Transmission electron microscopy (TEM) was performed using a JEM-200 transmission electron microscope (JEOL, Japan). Dynamic light scattering (DLS) and zeta potential data were recorded on a Zetasizer Nano ZS90 Nanometer particle size potentiometer (Malvern, Britain). Fourier transform infrared (FT-IR) spectra were recorded on a SPECTRUM ONE FTIR Spectrometer (America). The fluorescence spectra were obtained from the RF6000 spectrometer (Shimadzu, Japan). X-ray photoelectron spectroscopy (XPS) measurements were performed on a JSM6510LV instrument (Jeol, Japan). Circular dichroism (CD) spectra were measured on a Chirascan Series Spectrometer (Applied Photophysics, Britain). Isothermal titration

calorimetry (ITC) curves were obtained from TA Instruments-Waters LLC (America). The confocal laser images were performed on HGY08 LSM 900 confocal laser scanning microscopy (CLSM) (Zeiss, Germany).

## 1.2 Synthetic procedures and methods.

**Synthesis of TD-COFs.** The spherical TD-COFs was synthesized according to the reported method.<sup>[1-3]</sup> In detail, a centrifuge tube was preloaded with 1,3,5-tris(4-aminophenyl) benzene (TPB, 0.04 mmol) and 2,5-dihydroxyterephthalaldehyde (DHTP, 0.06 mmol). Then 5 mL of ACN was added to the tube and sonicated for 5 min to dissolve the building blocks completely. After that, HAc solution (0.7 mL 12 mol·L<sup>-1</sup>) was quickly added to the tube and immediately vortexed 1 min. After the solution stood at room temperature for 12 h, yellow precipitates were obtained. The collected yellow precipitates were washed with MeOH 3 times. Finally, the TD-COFs product was dried at 37 °C in a vacuum for 48 h, and then the TD-COFs were obtained.

**Synthesis of SP-COFs.** The spherical SP-COFs was synthesized as follows. The dry TD-COFs powder was sealed with 0.12 mmol POCl<sub>3</sub> in 5 mL anhydrous ACN at room temperature overnight for phosphorylation.<sup>[4]</sup> Subsequently, the product was alternately centrifuged with ACN 3 times to remove the unreacted POCl<sub>3</sub>. After that, the yellow powder was further hydrolyzed with NaOH aqueous solution to obtain the raw SP-COFs. The raw SP-COFs were further rinsed by MeOH which was used to remove the adsorbed solvents and impurities. Finally, the SP-COFs were obtained after activation at 37 °C in a vacuum for 48 h. It is worth noting that methanol activation is crucial to obtaining SP-COFs with high surface areas and reasonable pore size distribution. The activation process is as follows: the products of the room temperature reaction were isolated and collected by atmospheric filtration; the precipitated solids were rinsed with MeOH and then activated in a vacuum.

**Aβ<sub>42</sub> Pretreatment.** HFIP-pretreated peptides were used to obtain a homogeneous, aggregate-free preparation.<sup>[5]</sup> This step is necessary because pre-formed aggregates

induce rapid aggregation of amyloidogenic A $\beta$ <sub>42</sub>, which results in poor reproducibility among experiments. To treat the peptides with HFIP, pre-chill the HFIP container on ice inside a fume hood wearing adequate protection (HFIP is volatile and toxic). Add HFIP to pre-chilled tubes containing peptide lyophilizes to obtain a nominal peptide concentration of 0.5 mM. Sonicate the peptide solutions in a water-bath sonicator for 5 mins at room temperature. Vortex gently and incubate the tubes for 30 mins at room temperature. Remove HFIP by freeze-drying. The final product will be a peptide film at the bottom of the microfuge tubes. Dry peptide films were kept at -20 °C until use.

**Fibrillation Assay and ThT Fluorescence Monitoring.** The HFIP-pretreated monomers of A $\beta$ <sub>42</sub> (50  $\mu$ M) were dissolved in 50  $\mu$ M PBS buffer containing 0.02% NaN<sub>3</sub> (accelerated aggregation) and incubated in a water bath at a constant temperature of 37 °C for fibrillation kinetics assays in the presence or absence of TD-COFs and SP-COFs (60  $\mu$ g·mL<sup>-1</sup>).<sup>[6]</sup> ThT fluorescence was used to monitor the kinetics of A $\beta$ <sub>42</sub> fibrillation. At different time intervals, aliquots of the aggregating solutions were taken out for ThT fluorescence measurements. 30  $\mu$ L of the aggregating solutions were mixed with 240  $\mu$ L of 10  $\mu$ M ThT in 50  $\mu$ M PBS, pH 7.40, at different time points. The fluorescence was measured at  $\lambda_{ex}$  = 437 nm and  $\lambda_{em}$  = 485 nm. The data are presented as mean (3 independent experiments).

**The binding specificity of SP-COFs.** 50  $\mu$ M amino acid (13 amino acids. hydrophobicity: Ala, Phe, Met; hydrophilicity: Asn, Tyr, Gly, Ser, Thr, acidity: Asp, Glu, alkalinity: Lys, His, Arg) was added to the SP-COFs&A $\beta$ <sub>42</sub> co-incubation system respectively. The fibrillation kinetics curve was monitored with ThT in a water bath at a constant temperature of 37 °C. ThT was cultured in the polymerization solution for 12h, and the fluorescence value at 485nm was plotted for binding specificity assay. Similarly, in the co-incubation system without SP-COFs&A $\beta$ <sub>42</sub>, 13 amino acids were cultured and their ThT fluorescence kinetics curves were also measured.

**TEM and DLS measurements.** The TEM and DLS experiments were performed with

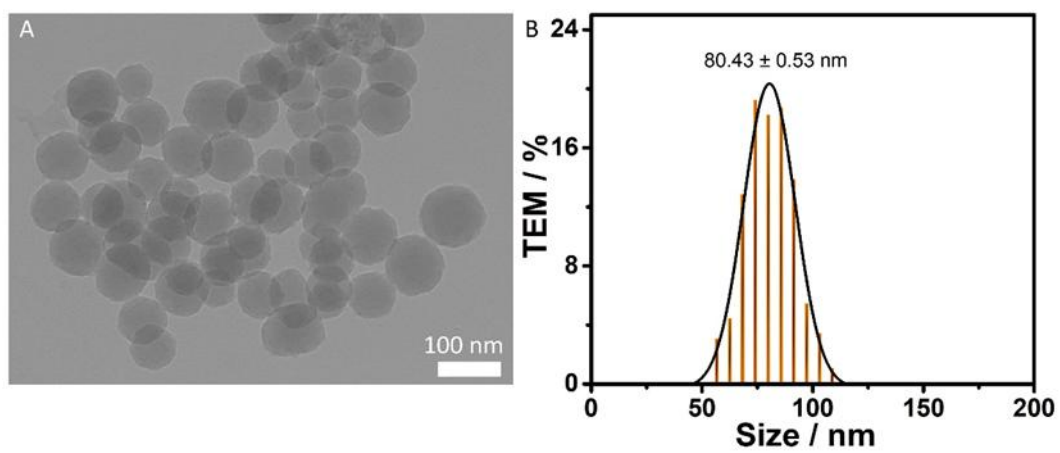
another aggregating solution (5  $\mu\text{M}$   $\text{A}\beta_{42}$  with 60  $\mu\text{g}\cdot\text{mL}^{-1}$  SP-COFs). In detail, 3  $\mu\text{L}$  aliquots from the aggregation reactions in the absence or presence of SP-COFs were diluted 10 times and spotted on carbon-coated Formvar grids to obtain TEM images at different time intervals. At the same time, the size distribution of scattering particles was recorded using a 2 mL aggregating solution. The control experiments were performed with  $\text{A}\beta_{42}$  alone.

**SP-COFs Inhibit Toxicity of  $\text{A}\beta_{42}$  in Cell Culture.** PC12 cells cultured in 1240 medium (5%  $\text{CO}_2$ , 37  $^\circ\text{C}$ ) were used to study the toxicity induced by  $\text{A}\beta_{42}$ . We tested whether SP-COFs protected cultured cells against toxicity induced by  $\text{A}\beta_{42}$ . We used the MTT (2  $\text{mg}\cdot\text{mL}^{-1}$ ) reduction assay for the measurement of cell viability.<sup>[7]</sup> Before initiating inhibition experiments, we tested whether SP-COFs were toxic to the cells (SP-COFs with varying concentrations: 5-60  $\mu\text{g}\cdot\text{mL}^{-1}$ ). By comparison, remarkable cytotoxicity was observed when  $\text{A}\beta_{42}$  (0-20  $\mu\text{M}$ ) was incubated with the PC12 cells alone. (The co-culture time of the above three experiments with cells was 48 h)

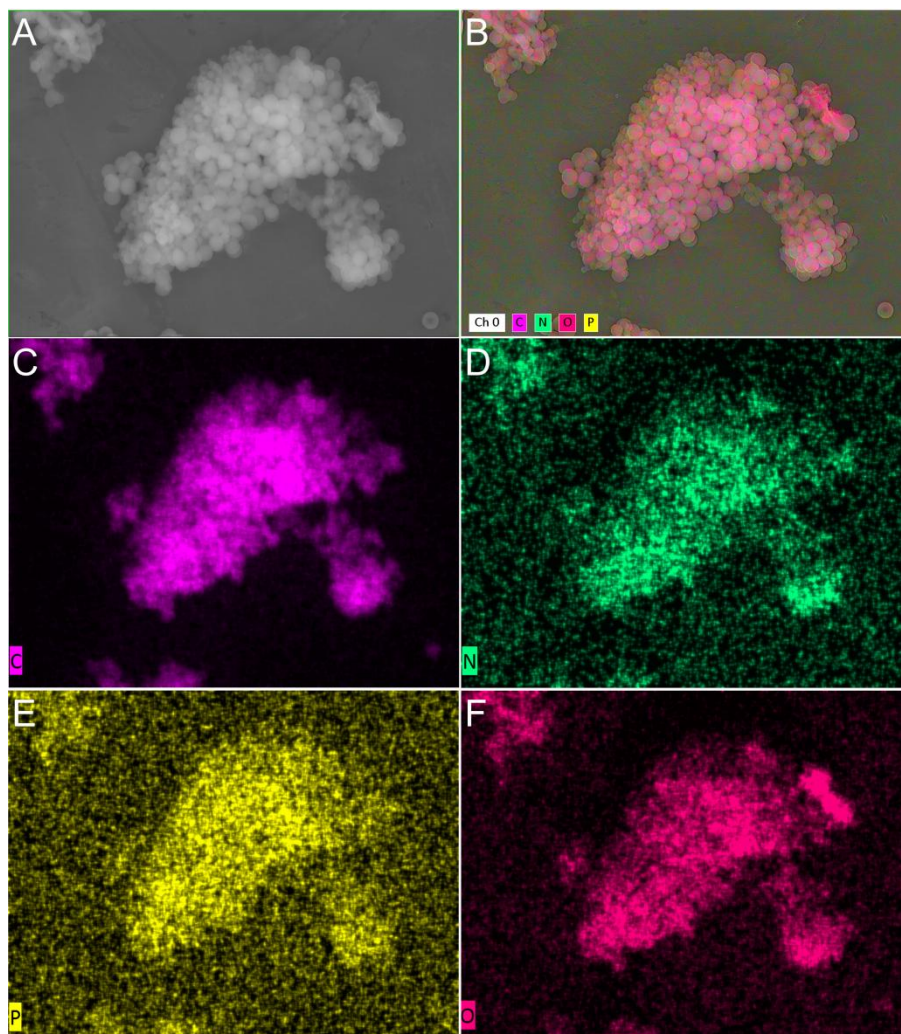
**The Confocal Laser Scanning Microscopy Images.** The images during the co-incubation of PC12 cells with SP-COFs and  $\text{A}\beta_{42}$  were investigated by confocal laser scanning microscopy (CLSM). We introduced a NIR fluorescent dye (stilbazolium derivative, 4-N, N-dimethylamino-4'-N-methyl-1,3-butadienyl]pyridinium dimer, synthesized by our lab) into SP-COFs to enable cell imaging through host-guest recognition.<sup>[8]</sup> The fresh SP-COFs (2 mg) were soaked in stilbazolium dye/ACN (10  $\mu\text{M}$ ) for 24 h, and then the product was alternately centrifuged with MeOH 3 times to remove the residual dye. After that, the yellow powder was further rinsed by MeOH which was used to remove the adsorbed solvents until the filtrate is colorless. Finally, the SP-COFs were obtained after activation at 37  $^\circ\text{C}$  in a vacuum for 48 h. The confocal laser images during the co-incubation of PC12 cells with SP-COFs were measured under the excitation of a 488 nm laser. SP-COFs were co-incubated with PC12 cells in the absence or presence of  $\text{A}\beta_{42}$  (5  $\mu\text{M}$ ) for 4 h.

**Molecular dynamics simulation.** Molecular dynamics simulation was done with Amber14 software. Molecular dynamics time: > 20 ns; Molecular dynamics requirements: A $\beta$ <sub>42</sub> peptide was completely stretched from one side of the pore of SP-COF to the other side in aqueous solution, and time nodes-structure phase of A $\beta$ <sub>42</sub> peptide across the single pore of SP-COFs in molecular dynamics process. The whole peptide system adopts gaff and ff14SB force fields, taking the A $\beta$ <sub>42</sub> peptide as the center, adding 10 Å cubic water box, and adding Na<sup>+</sup> to make the system electrically neutral. The topology and coordinate structure were saved and then carried out the simulation.

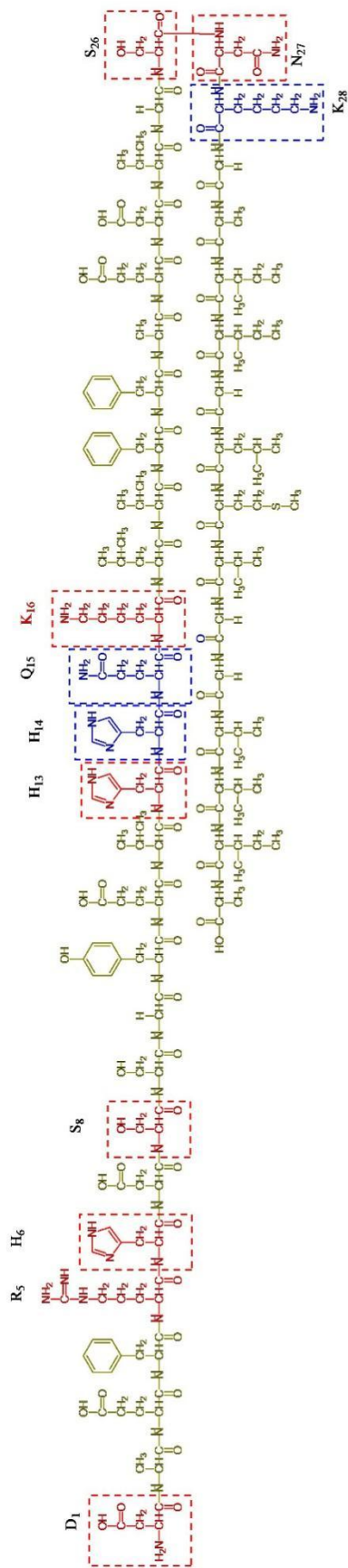
## 2. Figures and Tables



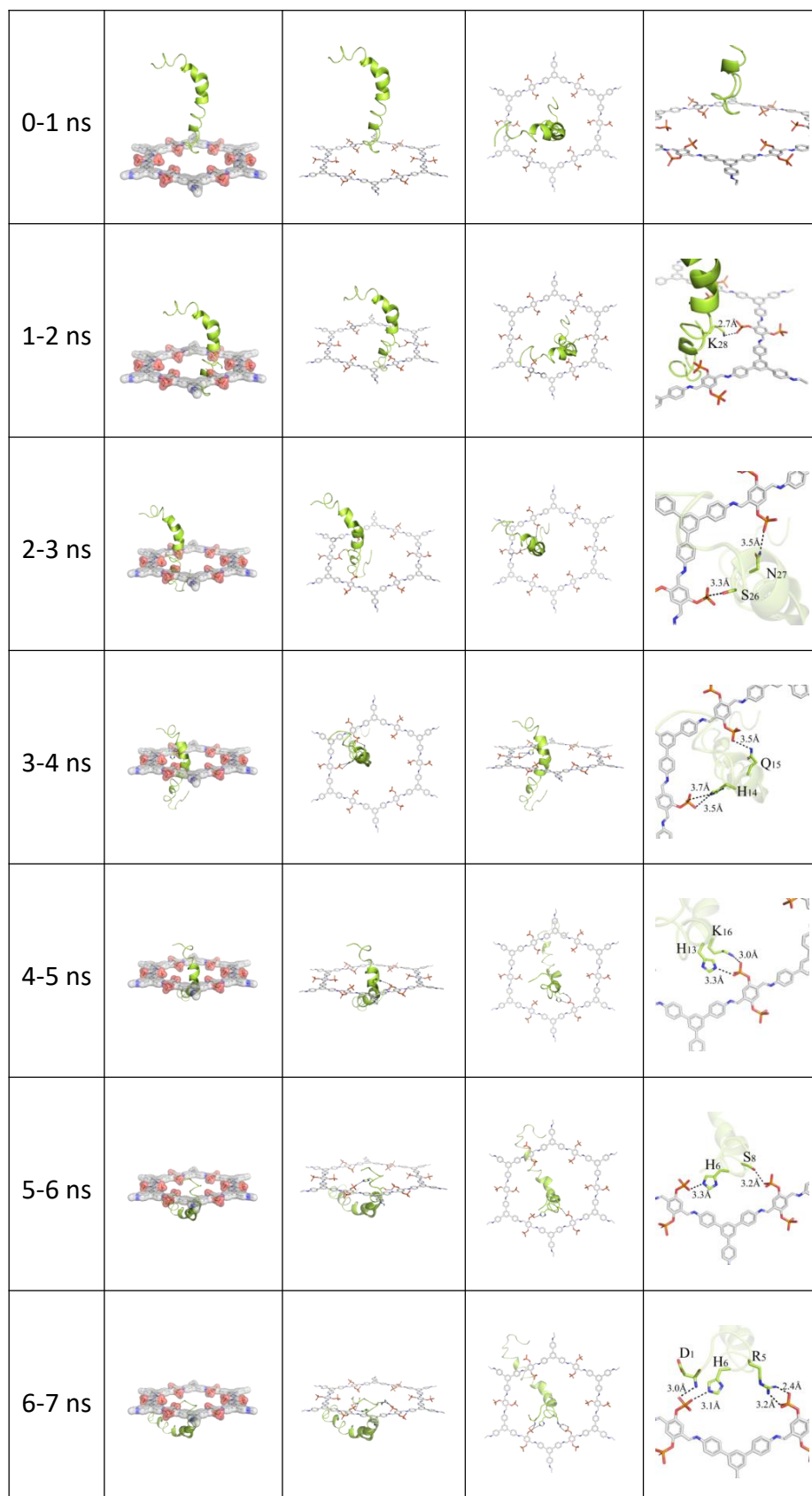
**Figure S1.** (A) TEM image and (B) particle size distribution of TD-COFs.



**Figure S2.** Energy-dispersive X-ray (EDX) spectroscopy of C, N, P, and O in SP-COFs.



**Figure S3.** The amino acid sequence and molecular structure of A $\beta_{42}$  peptide.



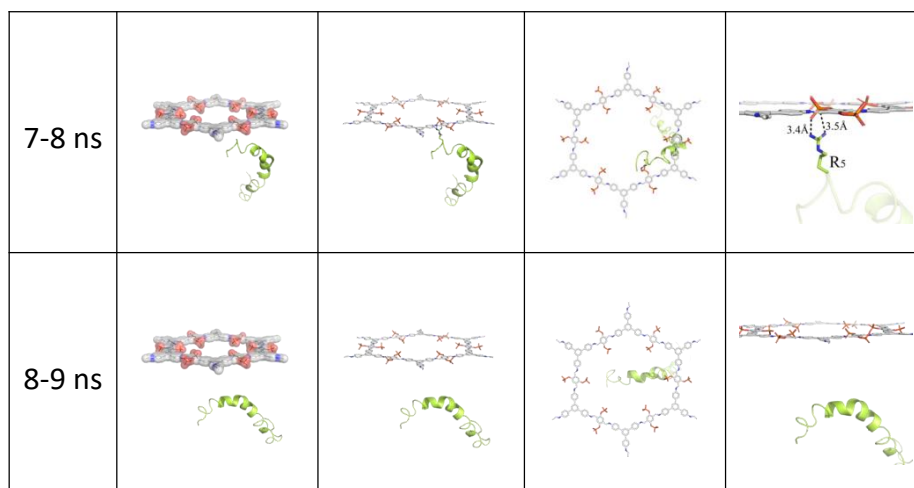


**Figure S4.** Time nodes-structure phase of A $\beta_{42}$  peptide across SP-COF (the single pore of SP-COFs) in molecular dynamics process.

**Noted:** The preformation of A $\beta_{42}$  peptide going through SP-COF is a holistic process, so the binding state between the two in real-time was monitored and nine structures were selected to display.

- (1) 0-1 ns: A $\beta_{42}$  has not yet had any contact with the SP-COF;
- (2) 1-2 ns: The head of A $\beta_{42}$  began to insert into the SP-COF and formed a polar interaction with SP-COF. Subsequently, a strong salt bridge between the lysine (K<sub>28</sub>) and phosphate group was formed. This action pulled A $\beta_{42}$  close to the SP-COF;
- (3) 2-3 ns: With A $\beta_{42}$  keeping entering the SP-COF, two hydrogen bonds were formed between asparagine (N<sub>27</sub>) and serine (S<sub>26</sub>) on the A $\beta_{42}$  chain and two phosphate groups on the inner pore of SP-COF, which maintained the contact between A $\beta_{42}$  and SP-COF;
- (4) 3-4 ns: When half of the body position of A $\beta_{42}$  (1/2 of the length) has entered the inner pore of SP-COF, histidine (H<sub>14</sub>) and glutamine (Q<sub>15</sub>) sites on the A $\beta_{42}$  chain formed three hydrogen bonds with phosphate groups on SP-COF;
- (5) 4-5 ns: Notably, nearly 3/4 of the body position of A $\beta_{42}$  (3/4 of the length) has passed through the inner pore of the channel of SP-COF, and a salt bridge was

formed among histidine (H<sub>13</sub>) and lysine (K<sub>16</sub>) sites and phosphate groups. This is conducive to the stable binding between A $\beta$ <sub>42</sub> and the inner pore of SP-COF;

- (6) 5-6 ns: A $\beta$ <sub>42</sub> has almost completely passed through the SP-COF. At this time, both salt bridge and hydrogen bond were formed between the histidine (H<sub>6</sub>), serine (S<sub>8</sub>) at the end of the A $\beta$ <sub>42</sub> chain, and the phosphate group on SP-COF;
- (7) 6-7 ns: The A $\beta$ <sub>42</sub> peptide has gradually passed through the SP-COF. Aspartic acid (D<sub>1</sub>) on the tail of A $\beta$ <sub>42</sub> formed a hydrogen bond with the phosphate group. Besides, histidine (H<sub>6</sub>), arginine (R<sub>5</sub>), and a phosphate group formed two salt bridges. These polarity effects made it difficult to dissociate A $\beta$ <sub>42</sub> from SP-COF;
- (8) 7-8 ns: The A $\beta$ <sub>42</sub> sequence completely passes through the inner pore of SP-COF. The salt bridge between arginine (R<sub>5</sub>) on the tail of A $\beta$ <sub>42</sub> and the phosphate group of SP-COF made A $\beta$ <sub>42</sub> and SP-COF suspended at the last moment, and maintained the final contact between them;
- (9) 8-9 ns: The A $\beta$ <sub>42</sub> sequence was completely passed through the SP-COF.

**Table S1.** Binding free energy of SP-COFs and A $\beta$ <sub>42</sub> complex (kcal/mol) and important polar residues.

Time note	Hydrophobic items	H-bonds items	Desolve energy items	Electrostatic items	Total energy	Interaction sites
0-1 ns	-1.03	-1.07	-1.12	-1.04	-4.26	-
1-2 ns	-0.69	-1.83	-1.11	-1.72	-5.35	K <sub>28</sub>
2-3 ns	-0.39	-1.94	-1.31	-1.89	-5.53	N <sub>27</sub> , S <sub>26</sub>
3-4 ns	-0.28	-1.95	-1.28	-1.9	-5.41	Q <sub>15</sub> , H <sub>14</sub>
4-5 ns	-0.34	-2.34	-1.26	-1.98	-5.92	K <sub>16</sub> , H <sub>13</sub>
5-6 ns	-0.43	-1.91	-1.21	-1.92	-5.47	S <sub>8</sub> , H <sub>6</sub>
6-7 ns	-0.29	-2.48	-1.24	-2.32	-6.33	H <sub>6</sub> , R <sub>5</sub> , D <sub>1</sub>
7-8 ns	-0.86	-1.6	-0.89	-1.34	-4.69	R <sub>5</sub>
8-9 ns	-1.35	-0.76	-1.11	-1.02	-4.24	-

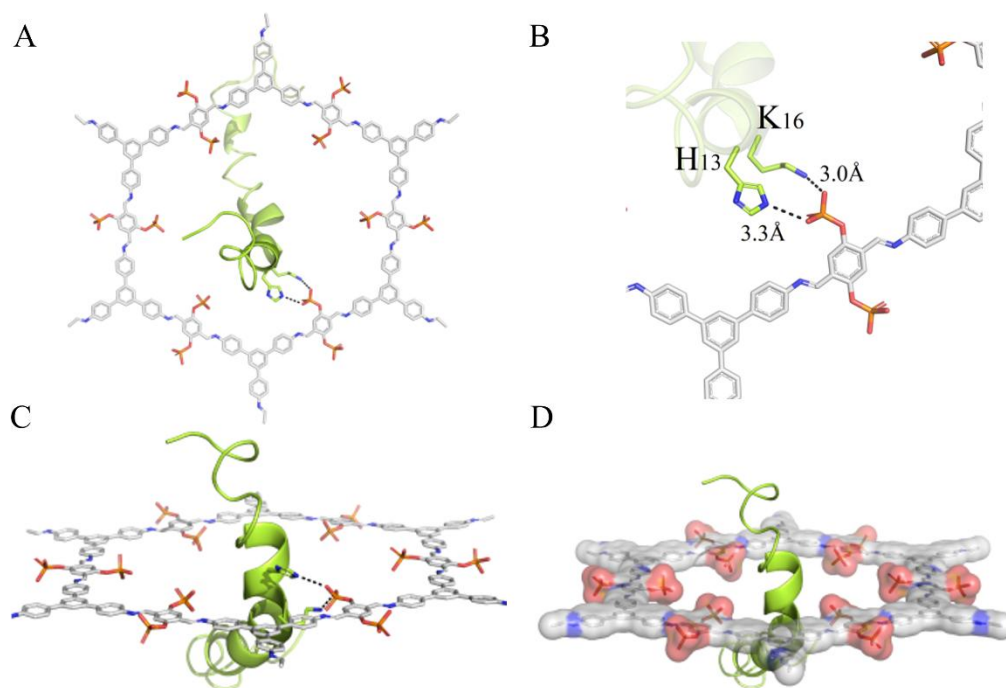


**Figure S5.** Steered molecular dynamics of the most stable phase (4-5 ns) of  $A\beta_{42}$  and single pore structure in SP-COFs during  $A\beta_{42}$  peptides pass through SP-COFs.

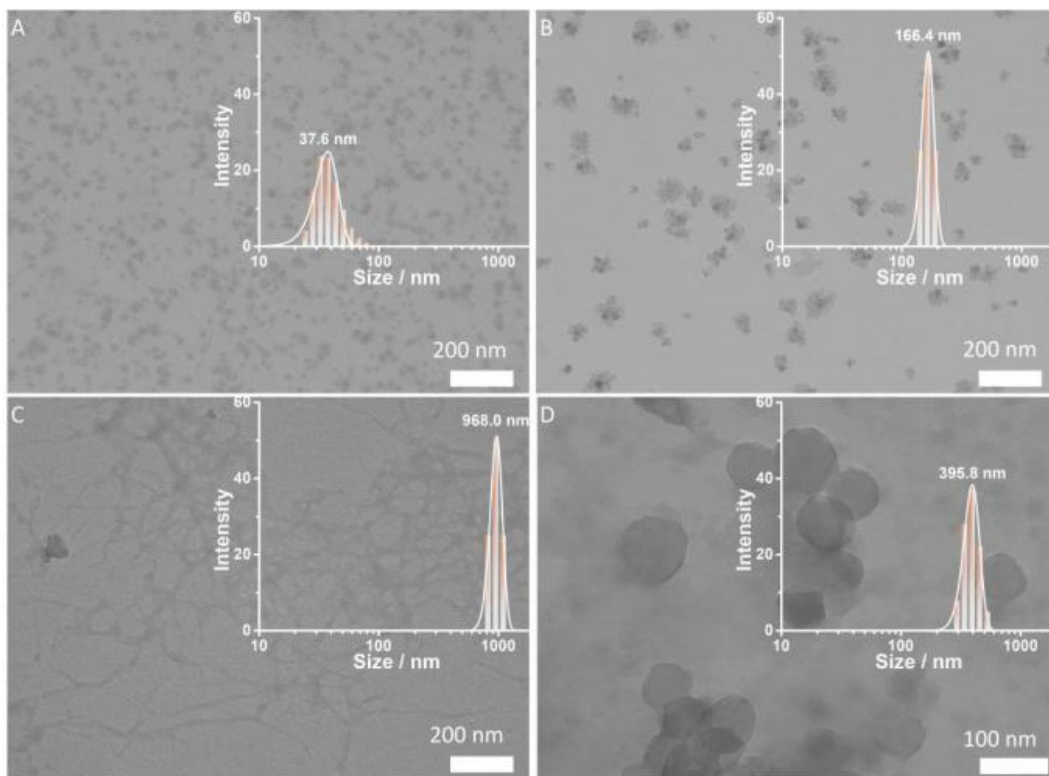


**Figure S6.** TEM images and DLS measurements of fibrillation time courses of  $A\beta_{42}$  ( $5 \mu\text{M}$ ).  $A\beta_{42}$  monomers were incubated at  $37 \text{ }^\circ\text{C}$  for 0 h (A), 24 h (B), and 96 h (C) in the absence of SP-COF nanospheres; (D)  $A\beta_{42}$  monomers were incubated at  $37 \text{ }^\circ\text{C}$  for 96 h in the presence (D) of SP-COFs ( $60 \mu\text{g}\cdot\text{mL}^{-1}$ ). Buffer:  $50 \mu\text{M}$  PBS,  $\text{pH} = 7.40$ .

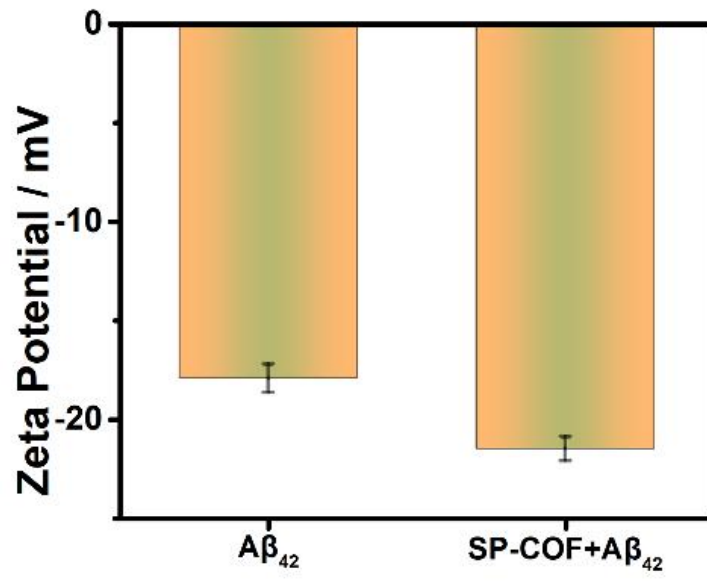
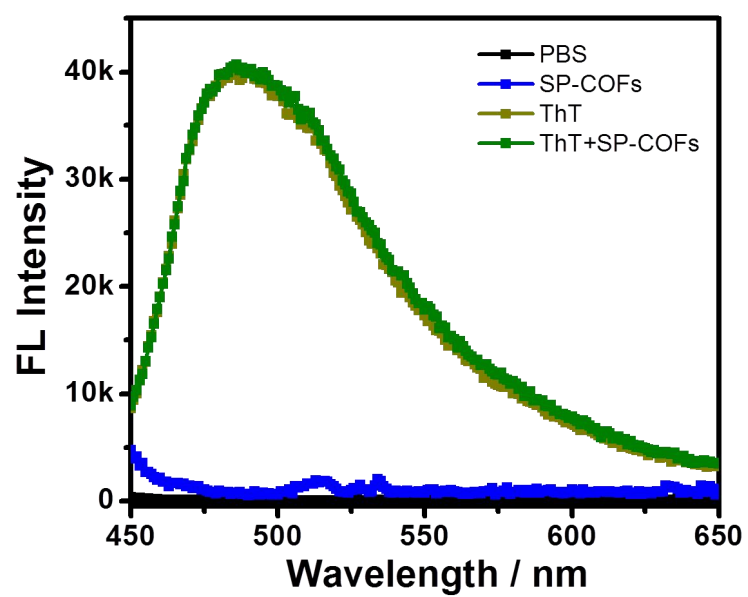
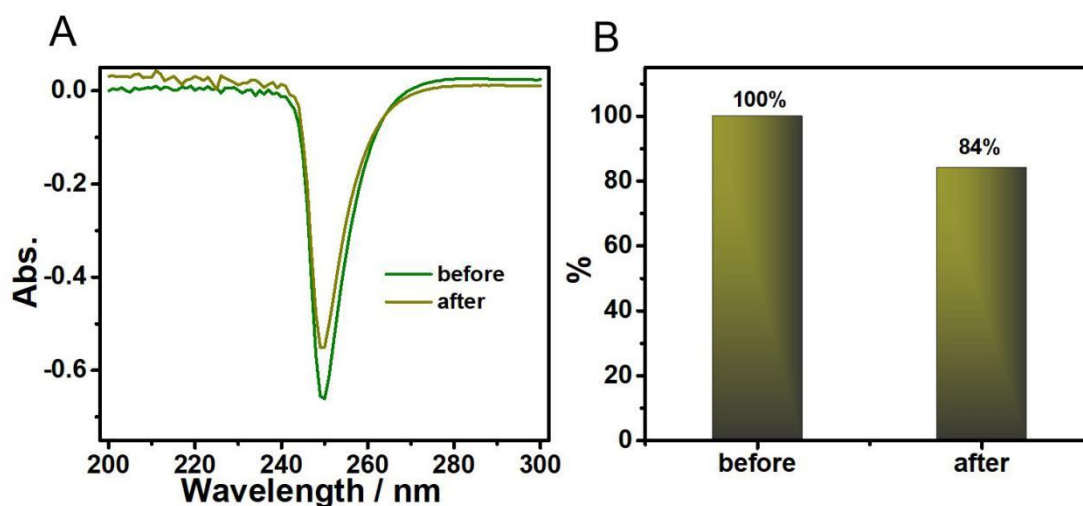


Figure S7. Zeta potential of Aβ<sub>42</sub> alone and co-incubation with SP-COFs.



**Figure S8.** Fluorescence spectra of SP-COFs, ThT, and their mixture in PBS buffer solution.



**Figure S9.** (A) The UV-Vis spectra of Aβ<sub>42</sub> (5 μM) before and after co-incubation (10 h) with SP-COF (60 μg·mL<sup>-1</sup>); (B) The change of peptide concentration before and after mixing of Aβ<sub>42</sub> (5 μM) and the SP-COFs (60 μg·mL<sup>-1</sup>).

**Note:**

We used UV-Vis absorption spectroscopy to explore the concentration changes of Aβ<sub>42</sub> before and after mixing with SP-COFs. According to the analysis of absorbance change, ca. 16.0 % of the protein was adsorbed by SP-COFs when they were mixed.

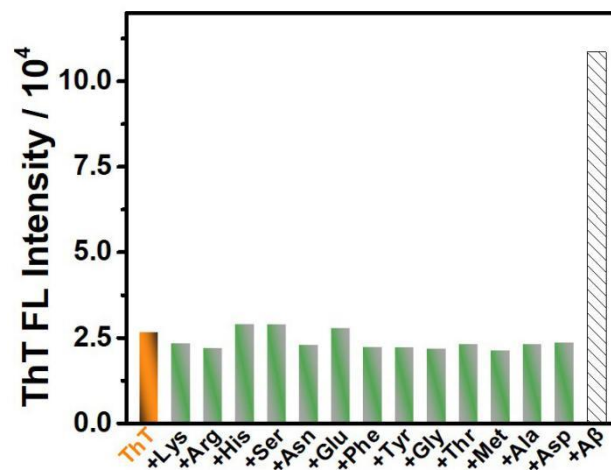


**Figure S10.** ThT fluorescence assay (co-incubate for 12 h) of A $\beta$ <sub>42</sub> or single amino acid (50  $\mu$ M, 10 times of A $\beta$ <sub>42</sub>).

**Note:**

The aggregation kinetic curves of the independent A $\beta$ <sub>42</sub> with amino acids were also adopted as control experiments to investigate the effect of surface properties on the A $\beta$ <sub>42</sub> fibrillation. Notably, the fluorescence intensity of ThT in the SP-COFs-free systems was no discernible difference by adding acidic amino acids, basic amino acids, and hydrophobic amino acids, as shown in Figure S10.

**Table S2.** The secondary structure content of A $\beta$ <sub>42</sub> according to the CD spectra.

Content (%)	A $\beta$ <sub>42</sub> /0 h	A $\beta$ <sub>42</sub> /24 h	A $\beta$ <sub>42</sub> /96 h	A $\beta$ <sub>42</sub> &SP-COF/96 h
<b>Helix</b>	19.9	1.3	8.1	4.3
<b>Antiparallel</b>	1.8	15.8	16.7	16.2
<b>Parallel</b>	5.9	4.1	12	4.6
<b>Turn</b>	25.4	21.2	16.3	21.9
<b>Others</b>	47.0	57.6	46.9	53.0

**Note:**

As shown in Table S2, the secondary structure contents of A $\beta$ <sub>42</sub> species including monomers (incubation for 0 h at 37 °C), oligomers (incubation for 24 h at 37 °C), and fibrils (incubation for 96 h at 37 °C), as well as the SP-COFs@A $\beta$ <sub>42</sub> co-culture system (co-incubation for 96 h at 37 °C) were quantitatively analyzed by BeStSel webserver. In the oligomerization process in 0 to 24 hours, the main change in the secondary structure of A $\beta$ <sub>42</sub> is that the helical structure is significantly reduced (19.9 % to 1.3 %), the antiparallel structure is significantly increased (1.8 % to 15.8 %), the configurations of parallel and turn are not significantly changed, and the "other" is significantly increased (47.0 % to 57.6 %). In contrast, from 24 hours to 96 hours, it is a fibrotic process, which is mainly characterized by the increase of parallel configurations (4.1 % to 12 %). The antiparallel configuration remained unchanged, and the turn decreased (21.2 % to 16.3 %), so the increase of helix was transformed from "others". Comparing the CD data of A $\beta$ <sub>42</sub> incubation for 96 hours in the presence and absence of SP-COFs, it can be found that the parallel configuration of A $\beta$ <sub>42</sub> in the presence of SP-COFs is significantly reduced (12.0 % to 4.6 %). The CD results strongly suggested that the SP-COFs could hinder the conformation transition of A $\beta$ <sub>42</sub> from  $\alpha$ -helical to  $\beta$ -sheet, confirming the interactions between A $\beta$ <sub>42</sub> and SP-COFs, which supports the conclusion that SP-COFs are process-specific inhibitors

of aberrant A $\beta$ <sub>42</sub> fibrillation.

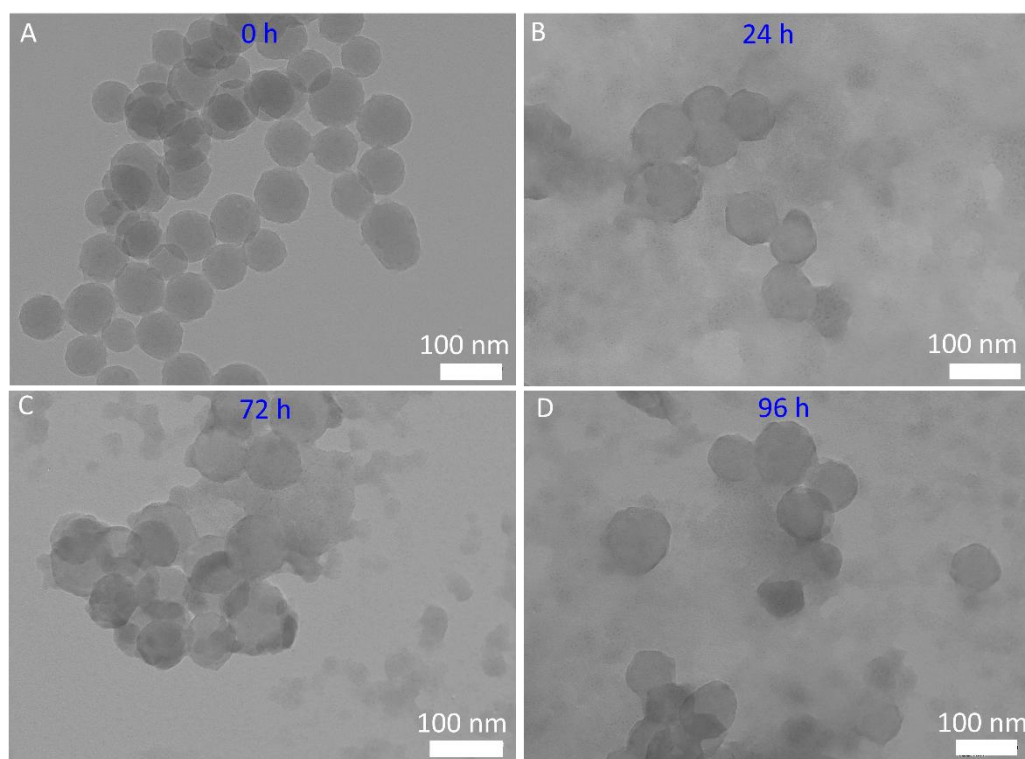


**Figure S11.** TEM images of SP-COFs after co-incubation with A $\beta$ <sub>42</sub> monomers at 37 °C for 0 h (A), 24 h (B), 72 h (C), and 96 h (D).

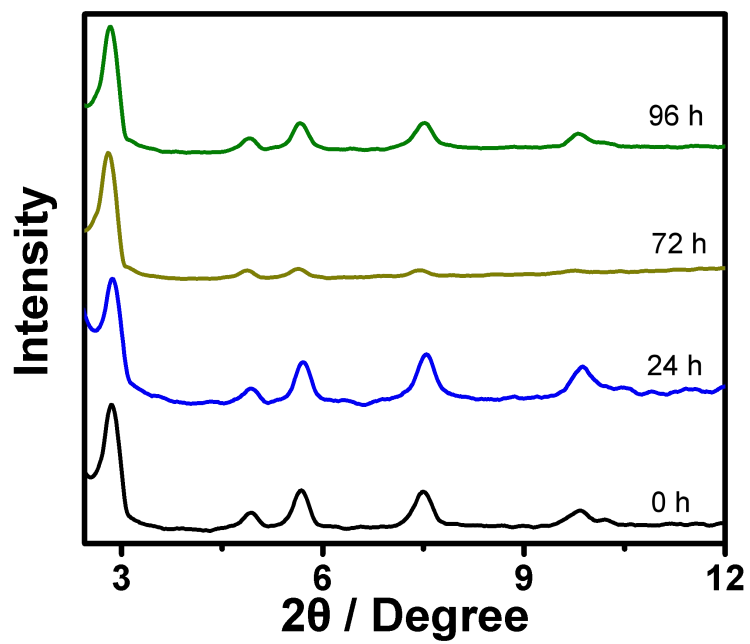


**Figure S12.** PXRD of SP-COFs after co-incubated with  $A\beta_{42}$  monomers in PBS buffer at  $37^\circ\text{C}$  at different intervals (0 h, 24 h, 72 h, 96 h).

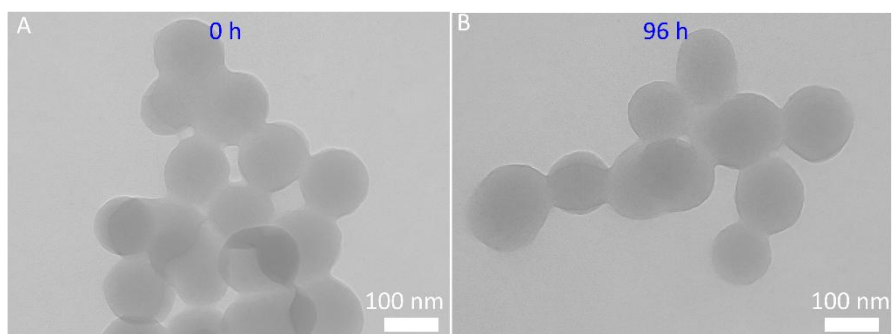


**Figure S13.** TEM images of SP-COFs were co-incubated in cell sap for 0 h (A) and 96 h (B).

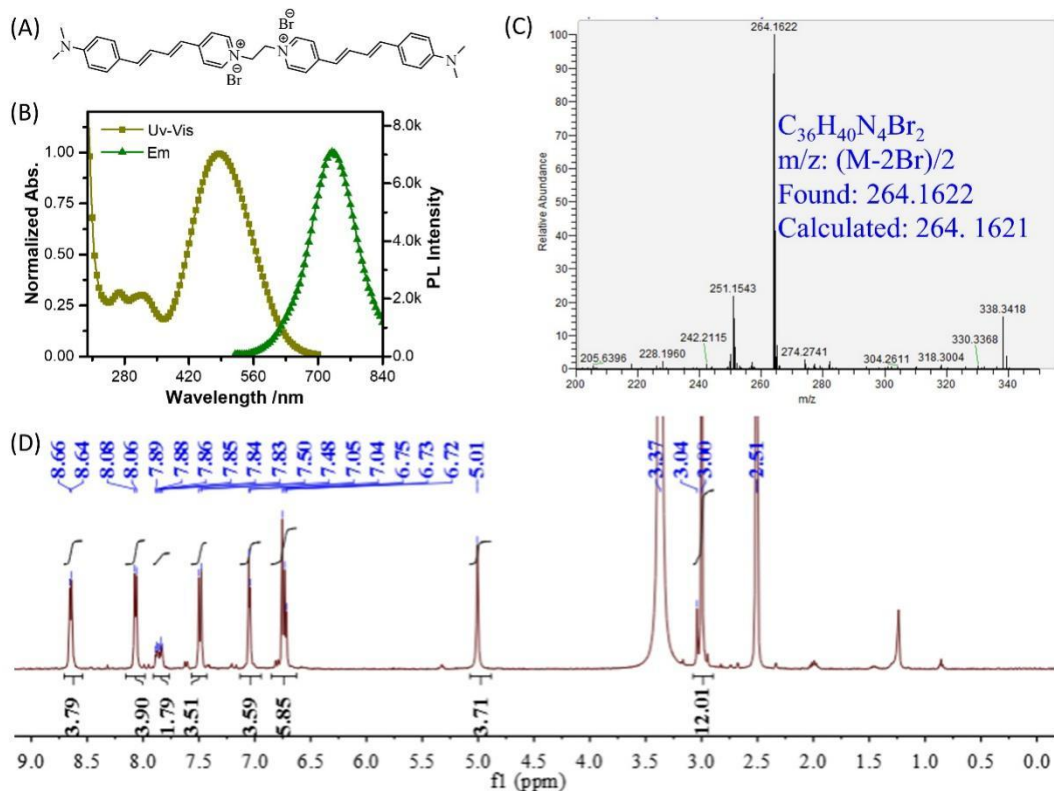


**Figure S14.** (A) Molecular structure, (B) UV-Vis and photoluminescence spectra, (C) mass spectrum (D) and  $^1\text{H}$  NMR (400 MHz,  $\text{DMSO-d}_6$ ) of the stilbazolium dye (4-N, N-dimethylamino-4'-N-methyl-1, 3- butadienyl] pyridinium dimer, DMBPD).

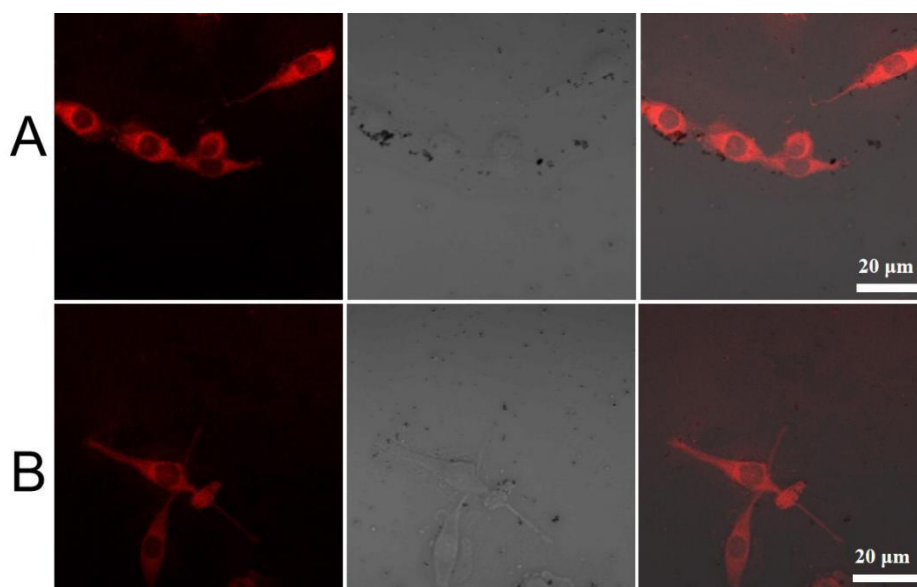


**Figure S15.** The CLSM images with excitation light of 488 nm of  $60 \mu\text{g}\cdot\text{mL}^{-1}$  DMBPD&SP-COFs. Darkfield (left), bright field (center), and superposition field (right).

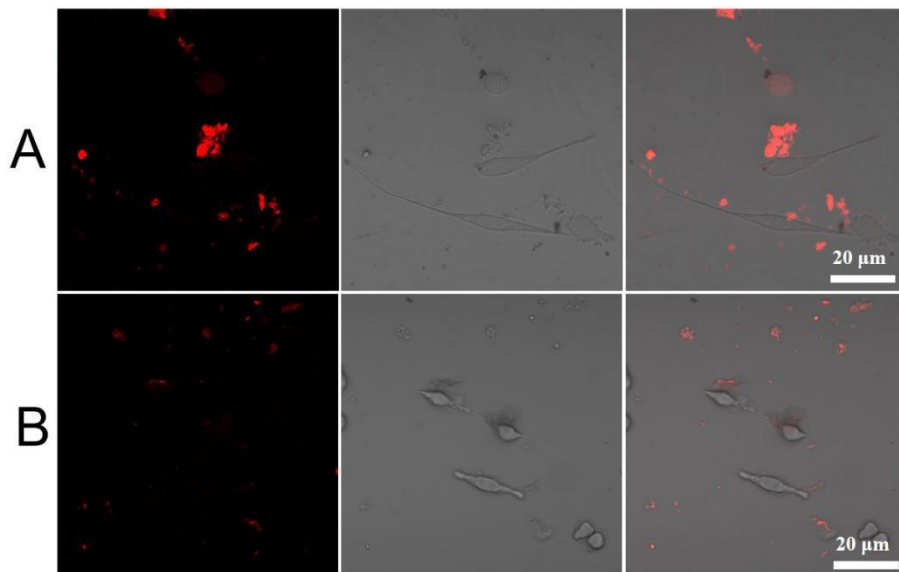


**Figure S16.** The CLSM images with excitation light of 488 nm of  $60 \mu\text{g}\cdot\text{mL}^{-1}$  DMBPD&SP-COFs and  $5 \mu\text{M}$   $\text{A}\beta_{42}$  (without labeling). Darkfield (left), bright field (center), and superposition field (right).

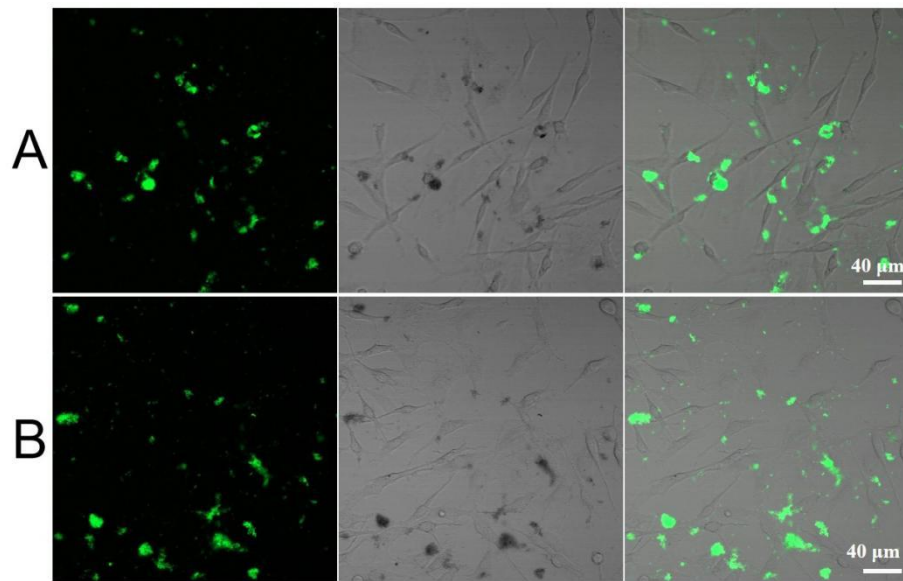


**Figure S17.** The CLSM images with excitation light of 488 nm of 5 μM FITC-Aβ<sub>42</sub>. Darkfield (left), bright field (center), and superposition field (right).

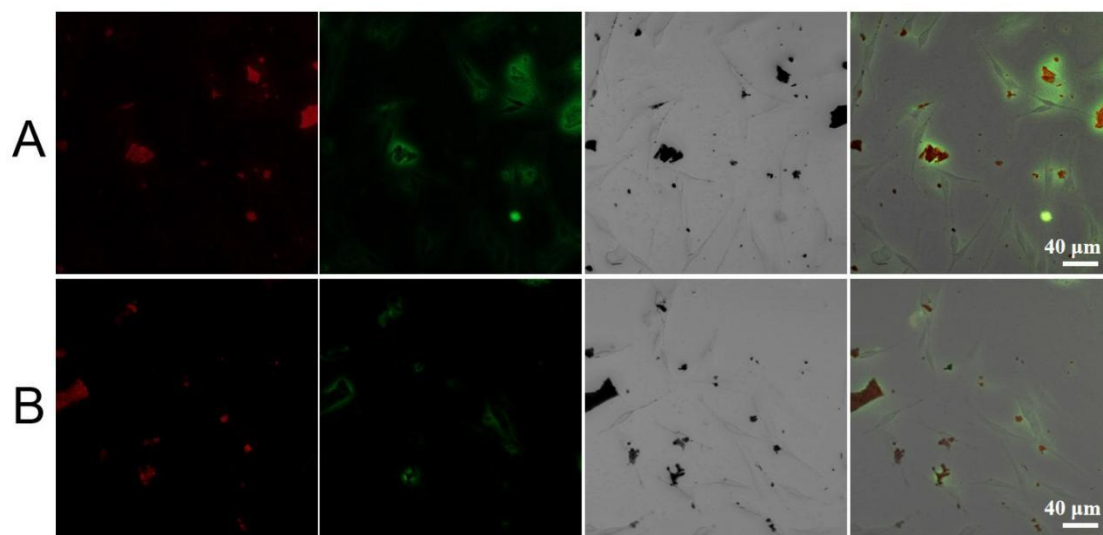


**Figure S18.** The CLSM images of  $60 \mu\text{g}\cdot\text{mL}^{-1}$  DMBPD&SP-COFs and  $5 \mu\text{M}$  FITC- $\text{A}\beta_{42}$  co-culture system with excitation light of 488 nm. Darkfield (two of left), bright field (center), and superposition field (right).

**Note:**

The cytotoxicity experiments of other three kinds of cells including Hela, HUVECs, and A549 cells were added to evaluate the effect of SP-COFs on cell viability and  $\text{A}\beta$ -induced cytotoxicity

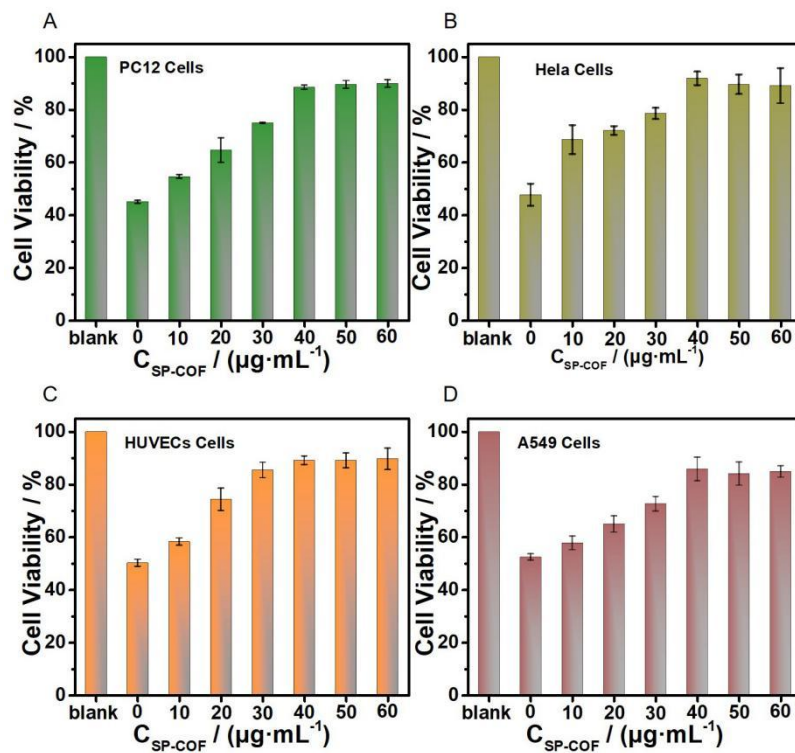


**Figure S19.** The cell viability was measured by a standard MTT assay. The viability of cells without any treatment for 48 h was specified as 100%. The PC12 (A), HeLa (B), HUVECs (C), and A549 (D) cells were preincubated with SP-COFs (0 – 60  $\mu\text{g}\cdot\text{mL}^{-1}$ ) and  $\text{A}\beta_{42}$  (5  $\mu\text{M}$ ).

## References

1. Ma, W., et al., *Size-Controllable Synthesis of Uniform Spherical Covalent Organic Frameworks at Room Temperature for Highly Efficient and Selective Enrichment of Hydrophobic Peptides*. *J. Am. Chem. Soc.*, 2019, **141**, 18271-18277.
2. Gong, S., et al., *Unravelling the Mechanism of Amyloid-beta Peptide Oligomerization and Fibrillation at Chiral Interfaces*. *Chem. Commun.*, 2019, **55**, 13725-13728.
3. Feriante, C.H., et al., *Rapid Synthesis of High Surface Area Imine-Linked 2D Covalent Organic Frameworks by Avoiding Pore Collapse During Isolation*. *Adv. Mater.*, 2020, **32**, e1905776.
4. Schwarz, D.M.C., et al., *A Phosphoramidate Strategy Enables Membrane Permeability of a Non-nucleotide Inhibitor of the Prolyl Isomerase Pin1*. *ACS Med. Chem. Lett.*, 2020. **11**, 1704-1710.
5. Sinha, S., et al., *Lysine-Specific Molecular Tweezers Are Broad-Spectrum Inhibitors of Assembly and Toxicity of Amyloid Proteins*. *J. Am. Chem. Soc.*, 2011. **133**, 16958-16969.
6. Richman, M., et al., *In Vitro and Mechanistic Studies of an Antiamyloidogenic Self-Assembled Cyclic d,l- $\alpha$ -Peptide Architecture*. *J. Am. Chem. Soc.*, 2013, **135**, 3474-3484.
7. Chung, Y.J., et al., *Carbon Nanodot-Sensitized Modulation of Alzheimer's  $\beta$ -Amyloid Self-Assembly, Disassembly, and Toxicity*. *Small*, 2017, **13**, 1700983.
8. Liu, Y., et al., *Molecular Weaving of Covalent Organic Frameworks for Adaptive Guest Inclusion*. *J. Am. Chem. Soc.*, 2018, **140**, 16015-16019.